

Estimation of shear-stress-induced endothelial nitric oxide production from flow-mediated dilation

Yoichi Yamazaki¹, Yohei Kondo² and Yoshimi Kamiyama³

Abstract—Vascular endothelial function assessment yields important diagnostic and prognostic information on patients with (or at risk of) cardiovascular diseases. Flow-mediated dilation (FMD) is the most widely used noninvasive method for assessing the endothelial function. In this method, the magnitude of FMD is used as a surrogate marker for the endothelial function. However, because vasodilation is affected by several other factors as well, the details of how this marker represents the endothelial function are not fully understood. Previously, we developed a mathematical model for vasodilation with intra- and intercellular pathways. In this study, we estimated the shear-stress-induced endothelial nitric oxide production from FMD measurements using the model. The results suggested that the accuracy of the estimated endothelial function obeys the characteristics of the shear stress added to the vascular wall. Furthermore, we showed that the FMD response describes not only the endothelial function but also vascular wall characteristics.

I. INTRODUCTION

Cardiovascular and circulatory system diseases are the major causes of deaths worldwide each year [1]. At the early onset of atherosclerosis, the bioavailability of atheroprotective agents such as nitric oxide (NO) decreases in the vascular wall. In addition, it has been found that the above-mentioned physiological behavior is closely related to many cardiovascular and circulatory system diseases besides atherosclerosis [2]. Therefore, using this physiological information, we can expect to realize the early diagnosis of cardiovascular diseases.

Flow-mediated dilation (FMD) refers to vasodilation in response to changes in shear stress during reactive hyperemia. FMD analysis is commonly known as an effective method to evaluate vascular endothelial function noninvasively. As the procedures, a cuff, which is placed below the transducer position, is inflated to produce ischemia in the forearm. The cuff is deflated after 5 minutes, and vasodilation of a longitudinal section of the brachial artery is measured by using the ultrasonic reflect-scope.

The magnitude of this shear-stress induced vasodilation is used as a surrogate marker for the endothelial function because the endothelium-derived NO production depends on the wall shear stress[3]. The FMD analysis has found favor

because it is non-invasive, repeatable, and can predict the extent of prognosis [4]. However, because the vasodilation in FMD is influenced by other factors as well, it remains unclear as to how effectively this marker represents the endothelial function in detail [5].

When a FMD analysis is performed, in addition to the FMD response, low-flow mediated constriction (L-FMC), which represents vasoconstriction at the low-flow state according to ischemia, is measured in some individuals. Recently, L-FMC measurements has been proposed as a novel assessment technique[5].

Because FMD and L-FMC are responses of the endothelial cell to the shear stress, more significant endothelial-function can be revealed by analyzing FMD and L-FMC data. We opine that this can be realized using a detailed mathematical model. To this end, we extended a model used for analyzing mechanical control of cation channels in the myogenic response [6] and developed a multiscale mathematical model of vasodilation with intra- and intercellular pathways.

In this study, we used blood flow velocity data obtained from the FMD analysis as the input to the proposed model and evaluated the expressibility of the model. In addition, we evaluated the effectiveness of the model in terms of endothelial function estimation.

II. METHOD AND MATERIALS

Endogenous NO is first synthesized in endothelial cells (EC) by the wall shear stress stimulation. The synthesized NO rapidly diffuses into neighboring the vascular smooth muscle, where it activates soluble guanylate cyclase (sGC), a heterodimeric hemoprotein. This activation catalyzes the conversion of guanosine triphosphate (GTP) into cyclic guanosine monophosphate (cGMP).

Acting as a second messenger, cGMP activates a family of cGMP-dependent protein kinases. This activation has two primary effects on the vascular smooth muscle: (1) a decrease in cytosolic Ca^{2+} concentration and (2) Ca^{2+} desensitization of the actinmyosin contractile system. Both effects ultimately lead to vasodilation.

We modeled the vasodilation mechanism in this study. Four separate models were integrated together to represent the FMD response. Fig. 1 shows the models and a schematic of their integration.

In the following subsections, we explain each model and its relationships with the other models.

A. NO Concentration Model

Fig. 1 shows the schematic description of this model. The NO concentration ($[NO]$) was computed according to the

¹ Y. Yamazaki is with the Knowledge Hub Aichi Priority Research Projects, Aichi Science and Technology Foundation, Toyota, Aichi, 470-0356, JAPAN. (telephone: +81-561-76-8388(ex.3079), e-mail: yamazaki@cis.aichi-pu.ac.jp)

² Y. Kondo is with the School of Information Science and Technology, Aichi Prefectural University, Nagakute, Japan.

³ Y. Kamiyama is with the School of Information Science and Technology, Aichi Prefectural University, Nagakute, Japan (telephone: +81-561-64-1111, e-mail: kamiyama@ist.aichi-pu.ac.jp).

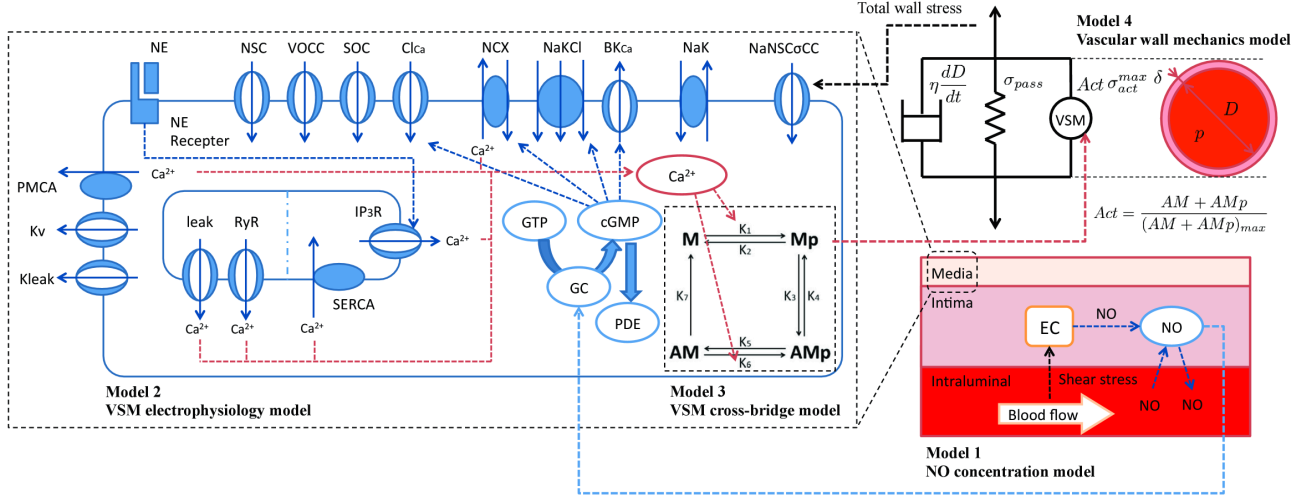


Fig. 1. Integrated multiscale model of FMD response showing the following four models: Model 1: NO concentration model; Model 2: Vascular smooth muscle (VSM) electrophysiology model with vessel stress-controlled channels [6]; Model 3: Four-state vascular smooth muscle cross-bridge model [10]; and Model 4: One-dimensional vessel wall mechanics model [6], [11].

following equation:

$$\frac{d[\text{NO}]}{dt} = R_{NO}(\tau) - \alpha_D[\text{NO}] \quad (1)$$

where $R_{NO}(\tau)$ is the endogenous NO production rate according to the wall-shear-stress τ , and α_D is coefficient corresponding to the NO diffusion rate.

The endothelial NO-concentration-rate model was proposed by Plata [7], and it is described by the sigmoid function as follows:

$$R_{NO}(\tau) = \frac{R_{NO,max}}{1 + \exp[-P_1\tau + P_2]} - R_{NO,min} \quad (2)$$

where $R_{NO,max}$ is the coefficient that represents the maximum NO production rate, P_1 and P_2 are the coefficients that determine the functions shape, and $R_{NO,min}$ is the coefficient that represents the minimum NO production rate.

B. Vascular Smooth Muscle Electrophysiology Model

The cytosolic Ca^{2+} concentration determines cross-bridge force generation and is governed by the influx of Ca^{2+} through the plasma membrane. Ca^{2+} induces Ca^{2+} release from the SR (sarcoplasmic reticulum), and the NO concentration acting on the vascular smooth muscle determines the buffering of Ca^{2+} in the cytosol.

The vascular smooth muscle electrophysiology model developed by Kapela et al. [8] was modified by Carlson [6], who added to it the functionality of hypothetical mechanically controlled channels. This model can be used for computing the dynamic state of the cytosolic Ca^{2+} concentration from the dynamic states of both the NO concentration and the total wall stress.

The NO concentration calculated using Model 1 was used as the input to the vascular smooth muscle electrophysiology

model. The resulting simulation analysis yielded evidence for NO diffusion in blood vessels and their neighborhoods [9].

The total wall stress calculated using Model 4 was used as the input for the mechanical channel part of the vascular smooth muscle electrophysiology model. The dynamic state of the mechanical channel governs three parameters. $\rho_{NaNSCoCC}^{max}$, $n_{NaNSCoCC}$, $\sigma_{50NaNSCoCC}$ are the maximum ratios of the σ -control to normal conduct, sensitivity to stress, and half-activation stress, respectively [6].

In this study, we used this electrophysiology model to construct the present model. We particularly examined the two abovementioned pathways, which are direct pathways for both vascular smooth muscle relaxation and contraction, and adjusted the related parameters.

C. Vascular Smooth Muscle Cross-Bridge Model

We used a four-state model of myosin binding and phosphorylation based on the vascular smooth muscle latch-state model by Hai [10]. Myosin can be of the following four types: free nonphosphorylated (M), free phosphorylated (Mp), attached phosphorylated (AMp), and attached dephosphorylated (AM). Fig. 1 describes the binding dynamics among states.

D. Vessel Wall Mechanics Model

In a one-dimensional description, the vessel wall is represented by the vessel wall viscosity term, nonlinear passive spring, and active stress generated by the vascular smooth muscle [6], [11].

From the above relationship, uniform changes in the vessel diameter (D) according to Act can be calculated as follows using Laplace's law:

$$\frac{dD}{dt} = \frac{D}{\eta} \left(\frac{PD}{2\delta_{wall}} - \sigma_{pass} - \text{Act} \cdot \sigma_{act} \right) \quad (3)$$

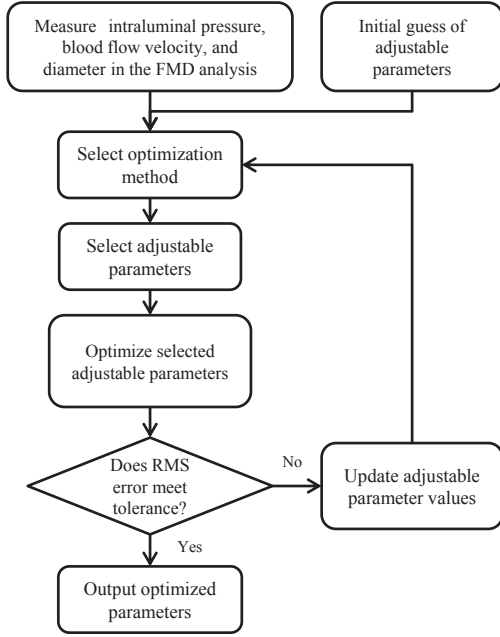


Fig. 2. Optimization protocol for adjustable parameters to fit proposed model to measurement data. All optimization methods determine the adjustable parameter value that minimizes the root mean square error between the estimated and measured diameters.

where P is the intraluminal pressure, δ_{wall} is the vessel wall thickness, σ_{pass} is the passive stress, σ_{act} is the maximally active stress, and η is the wall-viscosity coefficient.

The nonlinear passive stress (σ_{pass}) is a function of D and is given as follows:

$$\sigma_{pass} = \frac{{}^1C_{pass}}{\delta_{wall}} \exp \left[{}^2C_{pass} \left(\frac{D}{D_{rest}} - 1 \right) \right] \quad (4)$$

where ${}^1C_{pass}$ and ${}^2C_{pass}$ are adjustable parameters and D_{rest} is the passive diameter of the vessel under the intraluminal resting-position pressure. The maximally active stress (σ_{act}) can be expressed as a function of D as follows:

$$\sigma_{act} = \frac{{}^1C_{act}}{\delta_{wall}} \exp \left[- \left(\frac{D/D_{rest} - {}^2C_{act}}{{}^3C_{act}} \right)^2 \right] \quad (5)$$

where ${}^1C_{act}$, ${}^2C_{act}$, and ${}^3C_{act}$ are adjustable parameters. Vessel wall thickness (δ_{wall}) is given as follows:

$$\delta_{wall} = -\frac{D}{2} + \sqrt{\left(\frac{D}{2}\right)^2 + \delta_{wall,ref}(D_{ref} + \delta_{wall,ref})} \quad (6)$$

where D_{ref} is the luminal diameter and $\delta_{wall,ref}$ is the reference vessel wall thickness; these parameters decide the vascular wall area. In this study, these parameters are calculated from the ultrasonic image that we measured under the rest condition, as is shown in Table 2.

III. RESULTS

A. Optimization protocol

Adjustable parameters were determined to minimize the root mean square error. The root mean square error was computed as the difference in model response using the measured

TABLE I
TABLE OF ADJUSTED PARAMETERS.

Model 1		
Name	Unit	Estimated value
$R_{NO,max}$	nM/sec	348.525
P_1	cm ² /dyn	0.242
P_2	dimensionless	0.972
$R_{NO,min}$	nM/sec	95.658
Model 2		
Name	Unit	Estimated value
$\rho_{NaNSC\sigma CC}^{max}$	dimensionless	13.049
$n_{NaNSC\sigma CC}$	dimensionless	2.267
$\sigma_{50,NaNSC\sigma CC}$	N/m ²	55.652
NE	nM	378.156
Model 4		
Name	Unit	Estimated value
${}^1C_{pass}$	N/m	17.196
${}^2C_{pass}$	dimensionless	1.074
${}^1C_{act}$	N/m	21.847
${}^2C_{act}$	dimensionless	29.293
${}^3C_{act}$	dimensionless	16.829

TABLE II

TABLE OF FIXED PARAMETERS.

α_D	η (Pa · sec)	D_{rest} (cm)	D_{ref} (cm)	$\delta_{wall,ref}$ (cm)
1	1.5×10^5	0.38	0.38	0.053

blood flow velocity and measured diameter as inputs. The recursive processing terminates when the shrinkage of the root mean square error converges enough.

Fig. 2 shows the optimization protocol. The adjustable parameters were all the 13 parameters used in Model 1, Model 4, and the part of Model 2 relevant to the mechanical channel. We have listed these parameters in Table. 1. These parameters were chosen because the vascular wall structure has a considerable influence on them.

The model was coded in a JSim simulation environment (www.physiome.org). Optimizations were carried out by extending JSim optimization algorithms. The proposed names for models 2, 3, and 4 on the Physiome site were VSM_EphysPNaNSCSCC, VSM_4StateXB, and Vessel_Mechanics, respectively.

B. Numerical reproduction of FMD response

In FMD analysis, time profiles of the blood flow velocity and vessel wall diameter can be obtained from a healthy young subject, as is shown in Fig. 3. In this study, we performed parameterization by optimizing the proposed model for measured time profiles of Fig. 3. In this figure, the solid line denotes responses of the model with optimized parameters. The obtained adjustable parameters are listed in Table 1. Moreover, fixed parameters are listed in Table 2.

It can be seen from Fig. 3 that the model responses were reproduced well. This observation raises the possibility that the proposed model may be adequate for analyzing the FMD response.

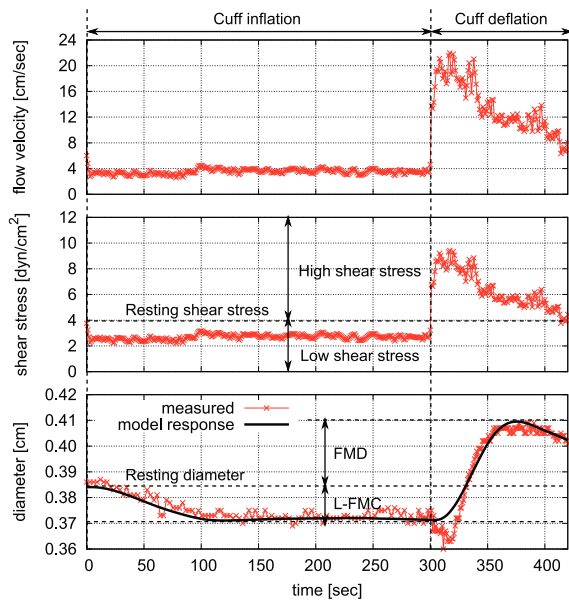


Fig. 3. Measured FMD assessment results and model response with adjustable parameters optimized by value. The crosses represent measured data and the solid line denotes the model response. The upper panel shows the input sequence, the middle panel shows variation of the shear stress, and the lower panel shows variation of the vascular diameter.

C. Evaluation of estimated physiological characteristics

Using Model 4, we calculated the Young's modulus to be 78.4 kPa considering intraluminal pressure under the rest condition. In contrast, the value of Young's modulus considering the young human artery is between 60 kPa and 80 kPa [12]. We can confirm that the obtained physiological characteristic of the vascular wall stress is valid on the physiological scale. Moreover, these parameters for the rat's vascular smooth muscle mechanical channel are within normal physiological range [6]. We can confirm that similar to the case of the vessel wall stress, the obtained vascular smooth muscle mechanical channel parameters are valid. The above results support the assertion that the obtained endothelial function has physiological validity.

The optimization was performed several times. We have recorded the result from each optimization and have presented the standard deviation in Fig. 4. In addition, the endothelial NO production rate which is calculated from Table 1 is shown in Fig. 4. We confirmed that the resting shear stress is the threshold of the phenomenon in which the standard derivation suddenly changes between the low shear stress domain (2 - 4 dyn/cm^2) and each other. As the reason, it is thought that the difference of added stimulation time between these domains strongly influences.

IV. CONCLUSION

In this study, we developed a mathematical model of vasodilation with intra- and intercellular pathways and analyzed the FMD response by combining four separate models.

We evaluated the estimation of the endothelial function using the model and confirmed that these results provide

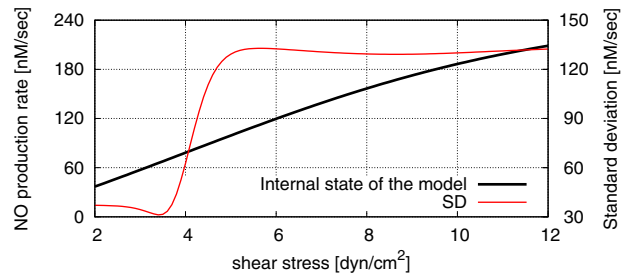


Fig. 4. Estimated endothelial NO production rate. The black solid line denotes the model response and the other line denote the standard deviation (SD).

two opinions for estimation of the endothelial function: (1) a unique estimation is possible under low shear stress and (2) estimation precision is related to the magnitude of shear stress.

In another respect, above opinions mean that the accuracy of the estimated endothelial function decreases in comparison with a case of the estimation including L-FMC when we estimate the endothelial function only from FMD response. Moreover, it supports that the model based analysis of FMD assessment data including both L-FMC and FMD provides more endothelial-function-related information.

REFERENCES

- [1] J. Loscalzo, "Endothelium, nitric oxide, and atherosclerosis: From basic mechanisms to clinical implications," *Circulation*, Vol. 102, No. 8, pp. e51-e51, 2000.
- [2] D. Santos-Garcia et al., "The role of flow-mediated dilation in ischemic stroke: time for action," *European Neurological Journal*, Vol. 2, No. 2, pp. 35-45, 2010.
- [3] C. Cheng et al., "Shear stress affects the intracellular distribution of enos: direct demonstration by a novel in vivo technique," *Blood*, Vol. 106, No. 12, pp. 3691-3698, 2005.
- [4] M. C. Corretti et al., "Guidelines for the ultrasound assessment of endothelial-dependent flow-mediated vasodilatation of the brachial artery: a report of the International Brachial Artery Reactivity Task Force," *J. Am. Coll. Cardiol.*, Vol. 39, pp. 257-265, 2002.
- [5] T. Gori et al., "Flow-mediated constriction: further insight into a new measure of vascular function," *Euro. Heart J.*, Vol. 32, pp. 784-787, 2011.
- [6] B. E. Carlson et al., "Mechanical control of cation channels in the myogenic response," *Am. J. Physiol. Heart. Circ. Physiol.*, Vol. 301, pp. H331-H343, 2011.
- [7] A. M. Plata et al., "Endothelial nitric oxide production and transport in flow chambers: The important of convection," *Annals of Biomedical Engineering*, Vol. 38, No. 9, pp. 2805-2816, 2010.
- [8] A. Kapela et al., "A mathematical model of Ca^{2+} dynamics in rat mesenteric smooth muscle cell: agonist and NO stimulation," *J. Theor. Biol.*, Vol. 253, pp. 238-260, 2008.
- [9] M. Kavdia et al., "Contribution of nNOS- and eNOS-derived NO to microvascular smooth muscle NO exposure," *J. Appl. Physiol.*, Vol. 97, pp. 293-301, 2004.
- [10] C. M. Hai et al., "Cross-bridge phosphorylation and regulation of latch state in smooth muscle," *Am. J. Physiol. Cell Physiol.*, Vol. 254, pp. C99-C106, 1988.
- [11] A. Kapela et al., "Multiscale FEM modeling of vascular tone: From membrane currents to vessel mechanics," *IEEE Trans. on Biomed. Eng.*, Vol. 58, No. 12, pp. 3456-3459, 2011.
- [12] T. Matsumoto, "Biomechanics of blood vessel walls: from macroscopic to microscopic viewpoint," *J. Jpn Coll Angiol*, Vol. 46, pp. 749-757, 2006.